EUROPEAN ORGANIZATION FOR NUCLEAR RESEARCH

CERN – A&B DEPARTMENT

AB-Note-2006-040 RF

A Structure for a Wide Band Wall Current Monitor

T. Kroyer

Abstract

In the framework of the EuroTeV programme a new wall current monitor for application in linear accelerators is currently being developed. A bandwidth of 20 GHz is aimed for in the new design. This note proposes an improved structure with very high bandwidth.

21st September 2006
Geneva, Switzerland

1 Introduction

The mission of the EUROTeV, a consortium of 28 European institutes is to develop the technology to realise the International Linear Collider. On the beam diagnostics side, a wide band wall current monitor (WCM) is currently under development at CERN. In order to accurately resolve single bunches with a spacing of 67 ps in the 3rd generation CLIC Test Facility (CTF3), a bandwidth of 20 GHz is required. The lower frequency limit of the WCM should be 100 kHz. At the location foreseen for the WCM the beam pipe diameter is 40 mm.

2 Review of previous designs

Most existing designs for monitoring the longitudinal beam profile rely on the concept of the resistive gap pick-up or wall current monitor [1, 2, 3, 4, 5]. In such a structure a load resistor R_0 is simply connected across a gap in the vacuum chamber. Fig. 1 shows a sketch of such a pick-up. At very low frequencies all the wall current will flow over the DC return path around the gap. In order to extend the bandwidth to lower frequencies, material with high permeability can be added around the inner tube of the coaxial section. This increases the impedance seen for the current that runs on the outer structure while not affecting the current that goes over the charge resistor R_0. With the ferrite loading acting like an inductor L, the low frequency limit is given by

$$\omega_L = \frac{R}{L}, \qquad (1)$$

where R is given by the parallel connection of the gap resistor R_0 and the characteristic impedance of the coaxial line. The low frequency limit can thus be tuned by adding an appropriate ferrite loading. In order to prevent problems with outgassing from the ferrites, a ceramic gap is often used so that the ferrites are separated from the beam vacuum.

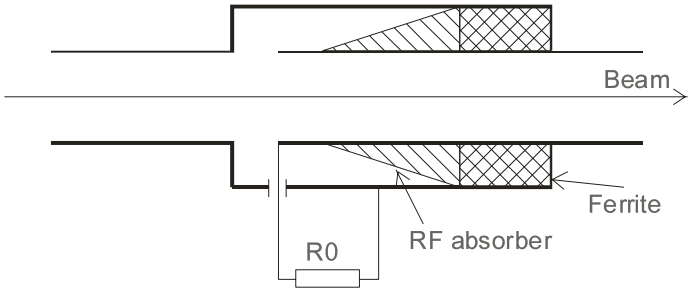

Fig. 1: A resistive gap pick-up. Depending on the design there may be only the RF absorber to damp high frequency resonances or only the ferrite to extend the bandwidth to lower frequencies.

The high frequency limit on the other hand is determined by the gap capacitance C as

$$\omega_H = \frac{1}{RC}. \qquad (2)$$

However, since the formula is based on quasi-static conditions is has to be used with care at very high frequencies. This "lumped-element" approach is strictly valid only when the distance between the individual elements is small compared to the wavelength. In the present case the relevant dimension is roughly the distance between the gap and the beginning of the feedthrough line, corresponding to the difference between the outer and inner pipe radii. Allowing a maximum distance of a tenth of the free space wavelength, we are in quasi-static regime for a

typical 5 mm tube spacing up to about c/(50 mm) = 6 GHz. For higher frequencies wave propagation around the corner between the gap and the beginning of the coaxial section has to be taken into account e.g. by using a full 3D simulation code.
Let's assume for the moment that Equation 2 is valid. In order to increase the bandwidth to high frequencies, C has to be made small. This can be achieved by decreasing the permittivity of the gap ε, e.g. by using a ceramic gap with low ε or no ceramics at all. Another way is to "eliminate" the gap capacity by changing the geometry.

3 Proposed structure

It is commonly known that for a charge moving at the speed v, in the limit $v = c$ the electric field is purely transverse. Fig. 2 shows an ultrarelativistic charge in a round metallic beam pipe. As in a TEM transmission line the electric field excited by the beam has only radial components. Now a very thin metallic coaxial pipe can be inserted without changing the field pattern, since the electric field is normal onto this cylinder. A part of the beam-induced field is "shaved off" and continues as a TEM wave in the coaxial structure. It can be picked with feedthroughs connected to the inner tube and used to diagnose beam properties. In the inner pipe the remaining beam field runs along undisturbed. Since, at least in the ideal case of a very thin inner tube, this structure does not change the field pattern, it should work in the same way for any frequency. Finite wall thickness will of course cause a certain field distortion which will show up as a ripple on the response which gets stronger for higher frequencies.

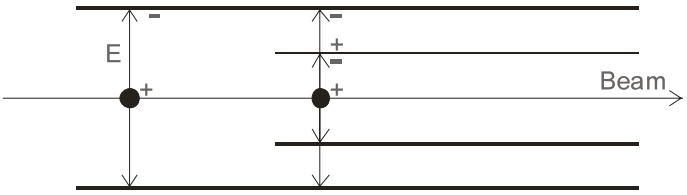

Fig. 2: Electric field pattern and induced charges for an ultrarelativistic charge entering a coaxial structure

Simulations

The properties of the proposed structure were evaluated using numerical simulations. In order to make the problem easier to handle the design was split into three regions, as depicted in Fig. 3. A cross-section change is needed to adapt the bigger outer beam pipe of the coaxial structure to the given aperture. The resulting structure can be thought of as a conventional WCM design with the gap smoothend out. It is also similar to the waveguide pick-up described in [6]. Another possibility is to have a continuous outer beam pipe and insert the inner pipe. This option has the advantage of avoiding the cavity-like cross-section change, but it reduces the beam aperture. This case is treated further down (geometry in Fig. 8).
The second section consists of the beginning of the inner pipe and the feedthrough. The feedthroughs themselves were modelled as coaxial 50 Ω lines without internal reflections. The feedthrough cross-section was chosen like the one described in [7]. Finally, the RF absorbers and ferrites in the coaxial line make up the third section. In a first approximation, each section can be analysed separately. Near-field effects between adjacent sections may be neglected this way.
After discussing the coaxial section, we are going to add the cross-section change to the geometry. Then the coaxial section plus feed-throughs are analysed and finally the whole design is simulated. The RF absorbers and ferrites are not studied as such; in the simulations, waveguide

ports acting as ideal RF absorbers were used. If not specified otherwise, the geometry parameters given in Tab. 1 were used in the simulations.

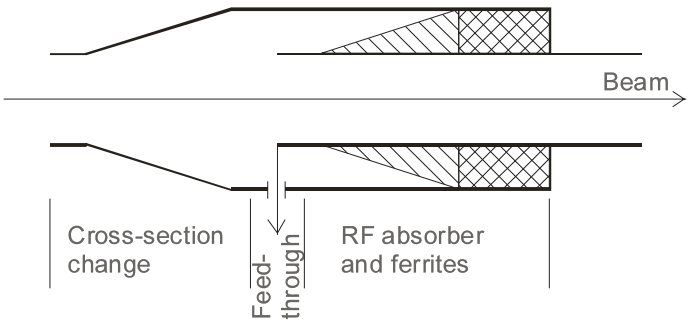

Fig. 3: The three sections of the WCM design. To some degree each section can be analysed separately.

Parameter	Symbol	Value [mm]
outer pipe radius	r_a	25
inner pipe inner radius	r_i	20
inner pipe thickness	t	1
length of tapering	l_t	50
feedthrough inner conductor radius	r_{fi}	0.4
feedthrough outer conductor radius	r_{fa}	0.92
wire radius	r_w	0.5

Tab. 1: Typical simulation parameters

Coaxial section

A Microwave Studio (MWS) simulation was set up to verify the properties of the coaxial structure. Fig. 4 shows the geometry used. As for the estimation above the values chosen for the outer and inner tube radii were r_a = 25 mm and r_i = 20 mm. The thickness of the inner tube was set to 1 mm; smaller values could be used to reduce the field distortion at the edge of the inner tube, but might in practice lead to mechanical problems. The gap between the two pipes is 4 mm wide. Since MWS cannot (yet) use particle beam to excite a structure, a 1 mm diameter wire was used instead of the beam. The geometry used and the results are shown in Fig. 4. The direction of the beam points to the right into the plane of the paper (Port 1). A TEM wave simulating the beam is excited at this side of the structure (Fig. 5). When it encounters the inserted tube, it splits up in two components while a fraction of the power is reflected (S_{11}). The major part of the power continues in the inner tube (S_{21}), while about -12.9 dB are coupled to the coaxial structure (S_{31}). The curve is almost flat up to at least 30 GHz. When r_i is varied, the coupling strength changes but the curve stays flat as in the present case.

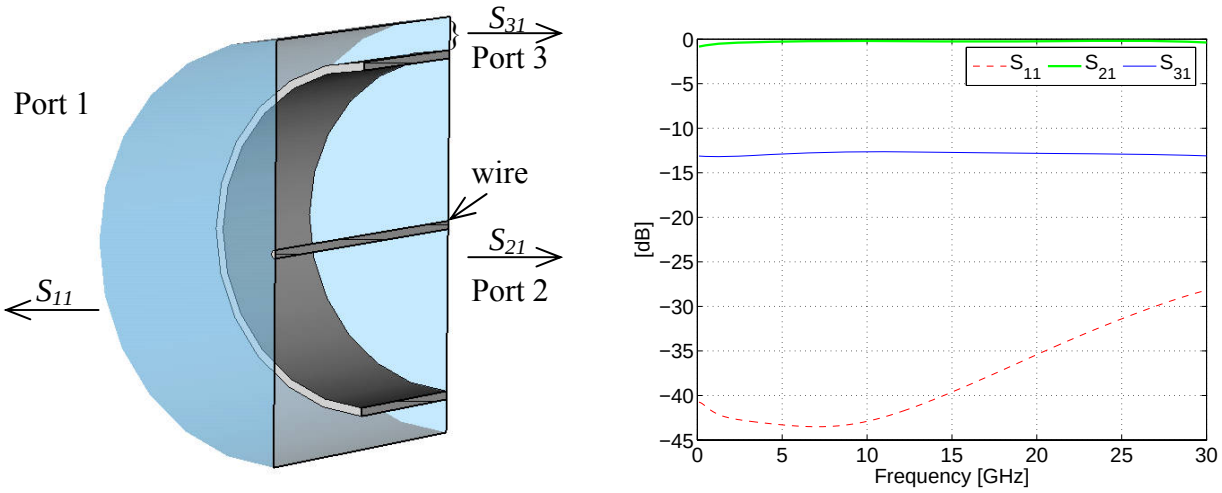

Fig. 4: Wire simulation of the coaxial structure with Microwave Studio. The beam going to the right into the plane of the paper is simulated by a 1 mm diameter wire. The signal coupled to the coaxial structure (S_{31}, solid blue trace) is very flat up to at least 30 GHz. In the model, air is represented in blue, conductors in grey and the background material is a perfect conductor.

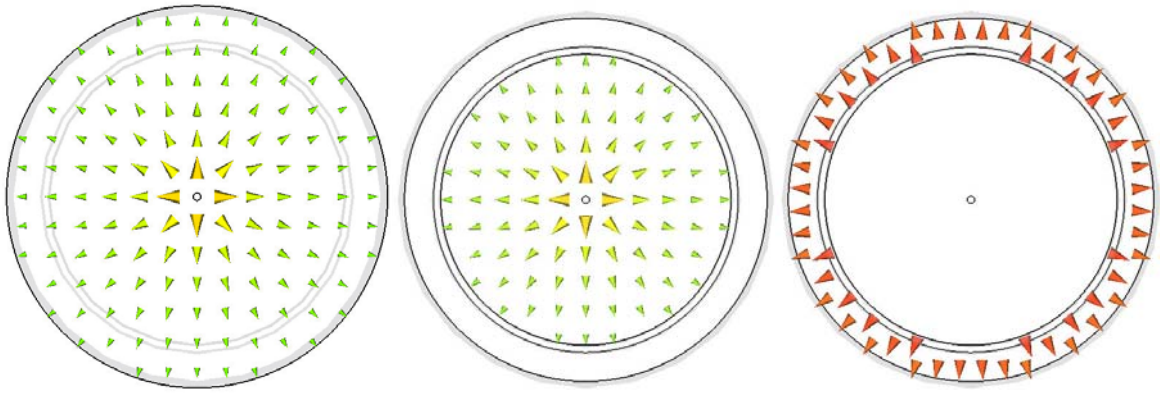

Fig. 5: Plot of the port modes' electric field. The incoming TEM wave (left) splits into a component running in the inner tube (S_{21}, center) and the desired pick-up component in the coaxial section (S_{31}, right).

Coaxial structure with tapering

In order to preserve the beam aperture at both sides of the WCM, a tapering before or after the coaxial structure is needed. The first case is illustrated in Fig. 6 (left). It is worthwhile to compare this structure with other designs described in the literature, e.g. in [3,4]. The diameters of the pipes in the two structures are the same, but the short longitudinal gap (Fig. 6, right) is replaced by a smooth transition (Fig. 6, left) .

Port 1 on the left side of each structure is excited with the TEM mode. The relevant parameter is S_{31}, the transmission to the TEM mode in the coaxial structure.

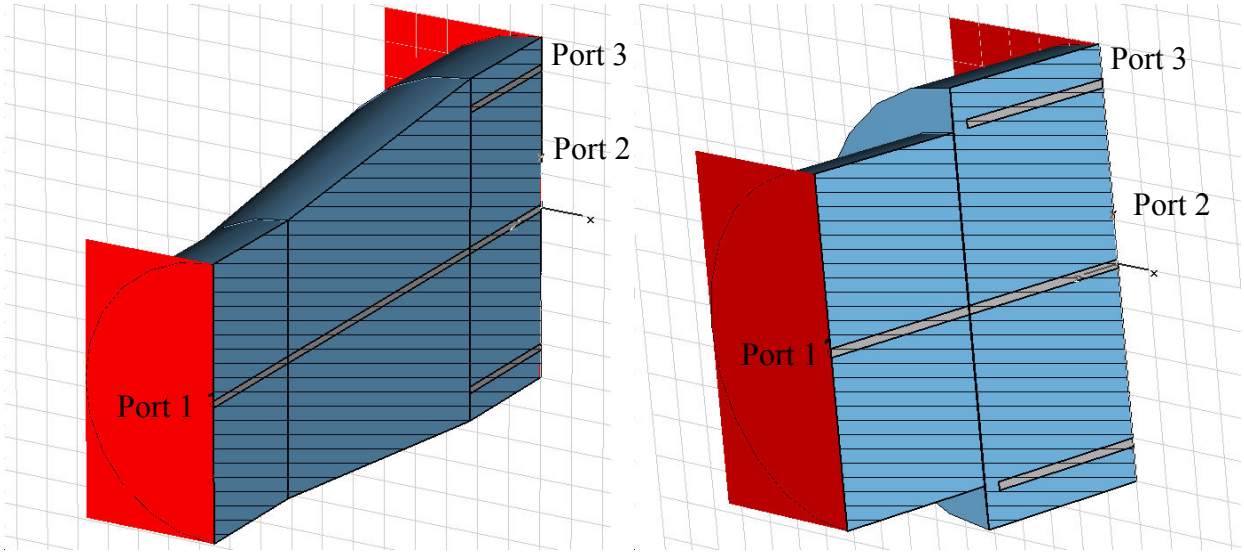

Fig. 6: Left: Geometry of the coaxial section with tapering. Right: A typical design from literature with 2 mm gap width.

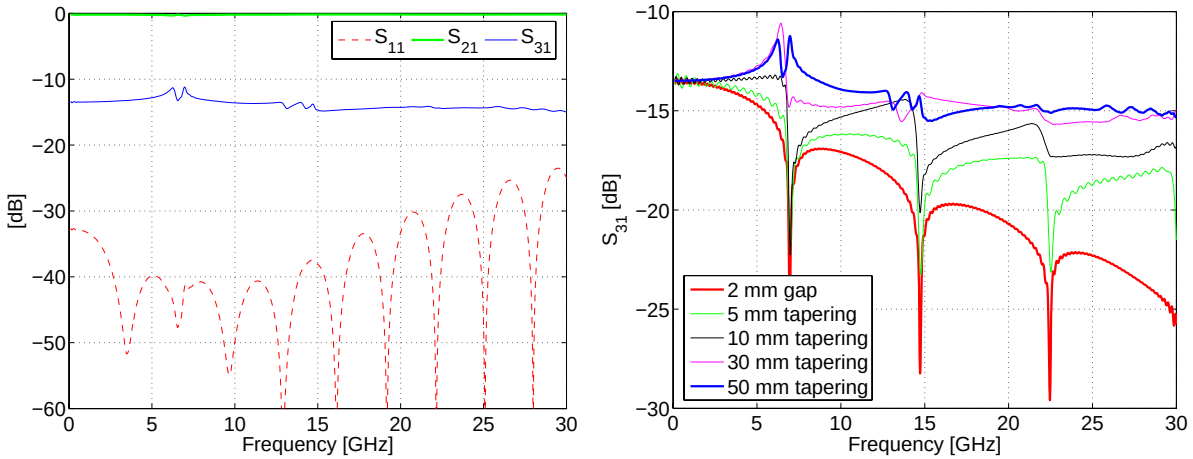

Fig. 7: Left: S parameters of the tapering combined with the coaxial section as sketched in the left of Fig. 6. Right: Transmission to the outer coaxial structure for different tapering lengths. The old design is obtained when the tapering length goes to zero and a small longitudinal gap is introduced. Please note that the feedthroughs are not included in the design, which in particular decreases the high-frequency cut-off of the design with 2 mm gap.

The left plot in Fig. 7 shows the S parameters obtained for a tapering length of 50 mm. The average magnitude of S_{31} did not change much compared to the data without tapering. However, resonances appear at the cut-off of the TM modes with rotational symmetry, i.e. TM_{01} at 6.9 GHz, TM_{02} at 14.7 GHz and TM_{03} at 22.4 GHz. Since a wire simulation is used, the cut-off frequencies are somewhat shifted up in frequency compared to a circular waveguide with 40 mm diameter.
In the right plot in Fig. 7 several structures with different taperings are compared. When the tapering length is decreased from 50 mm down to 0, leaving a 2 mm wide gap, a typical conventional WCM is obtained. Its response is plotted in the thick red curve. Due to the considerable gap capacity and the missing feedthroughs (high R) the power coupled to the coaxial structure decreases rather fast with frequency. At 20 GHz the response is about 6 dB below the structure with 50 mm tapering length (thick blue curve). For shorter taperings the intermediate curves were obtained.

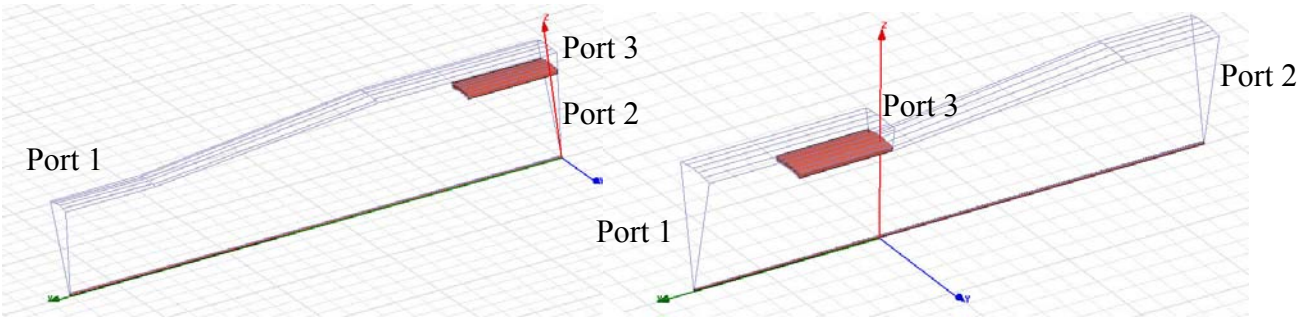

Fig. 8: Comparison between the WCM structure with tapering before (left) and after (right) the coaxial section. Vacuum is drawn as a wire frame, metal in orange. The structures are excited on the left side with a wire in TEM mode. The signal coupled to the coaxial structure is taken between the inner and outer pipe, on the right side in the left plot and in the center in the right plot. Only a sector covering 22.5° of the entire geometry was meshed.

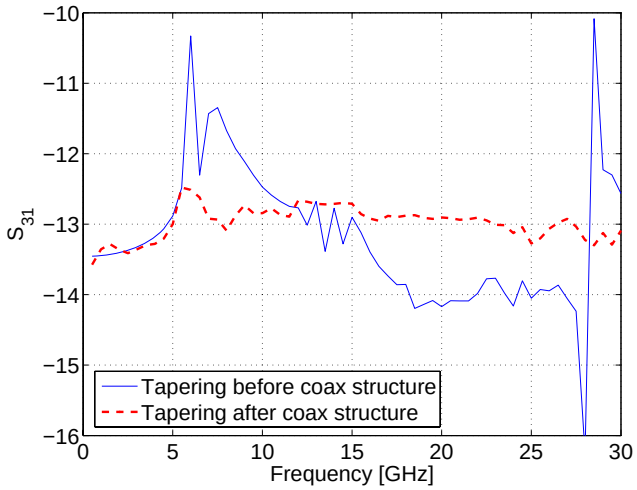

Fig. 9: Simulation results for the two structures shown in Fig. 8. With the tapering after the coaxial section trapped modes are avoided; the corresponding resonances disappear (orange trace).

Another interesting feature can be read from this plot. Common to all structures are resonances at the cut-off of TM_{0n} modes. However, when the tapering becomes longer, the sharp resonances start to split up and at some frequencies the coupling to the coaxial structure appears to be enhanced.

As an alternative option for tapering, if an aperture restriction can be tolerated, the inner pipe may be inserted into the beam pipe and a taper added after the coaxial section (Fig. 8). The design with the tapering before the coaxial section was compared to the one with tapering after it in HFSS simulations. The latter structure is advantageous for RF reasons, since higher order modes excited at the edge of the inner pipe can run back into the beam pipe without encountering discontinuities, at least as long as the beam pipe is uniform over a sufficient length. No trapped modes will thus appear.

Indeed, as shown in Fig. 9, the coupling to the coaxial structure is very flat up to 30 GHz for the second geometry.

Coaxial structure with feedthroughs

At some point the coaxial structure must be connected to the outside world. For this purpose feedthroughs are used that guide the signal out to a coaxial line. This feedthrough usually sits on

the beginning of the coaxial section. If it is moved backwards, resonances between the beginning of the coaxial line and the feedthrough are possible.
Fig. 10 shows the coaxial section with four feedthroughs around the circumference. In the center plot the electric field for the first azimuthal resonance is shown. The resonance condition is that the distance between two feedthroughs measured about halfway between the inner and outer pipe equals an integer multiple of the free space wavelength. For four feedthroughs, pipe radii of $r_i = 20$ mm, $r_a = 25$ mm and an inner wall thickness of 1 mm the first resonance appears at c/(2π*23/4 mm) = 8.3 GHz. This can also be seen in the simulation results for the signal coupled to one feedthrough (S_{41}, right plot of Fig. 10). The curve is flat up to about 5 GHz, then the proximity of the resonance starts degrading the response. For the present beam pipe diameter, in order to get an appreciably flat response up to 20 GHz about 16 feedthroughs are needed. The first azimuthal resonance is then pushed beyond 30 GHz.

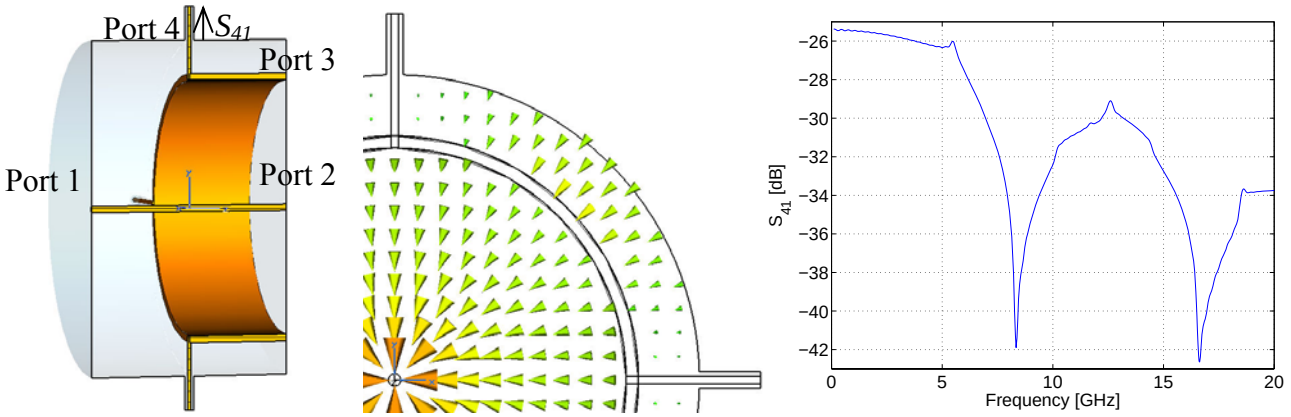

Fig. 10: Left: Four feedthroughs at the beginning of the coaxial section guide the pick-up signal out to a coaxial line. Center: When the distance between two feedthroughs becomes equals to the free space wavelength, the first azimuthal resonance appears in this structure (E field at first resonance plotted). Right: The signal coupled to one feedthrough (S_{41}) is flat up to about 5 GHz.

Coaxial structure with 16 feedthroughs

The geometry used for simulating the coaxial structure with 16 feedthroughs is shown in Fig. 11 along with electric field at 20 GHz. The corresponding S parameters are given in Fig. 12. The S parameters are all calculated using the incident power only in the given sector of the structure. For the whole structure S_{41} is what we would get after combining the outputs of all 16 feedthroughs. It is interesting to note that due to the addition of the feedthroughs S_{41} has decreased by about 6 dB in the lower frequency range (1 GHz) compared to Fig. 9, while S_{21} improved slightly. At about 5.5 GHz, 11.8 GHz and 17.9 GHz the TM_{0n} cut-offs cause resonances. Above 17 GHz S_{41} slowly starts to decrease. The fraction of the power that continues running down the coaxial section (S_{31}) tends to increase for higher frequencies due to power leaking through the feedthrough section. Apart from the resonances, the PU response is still pretty flat.

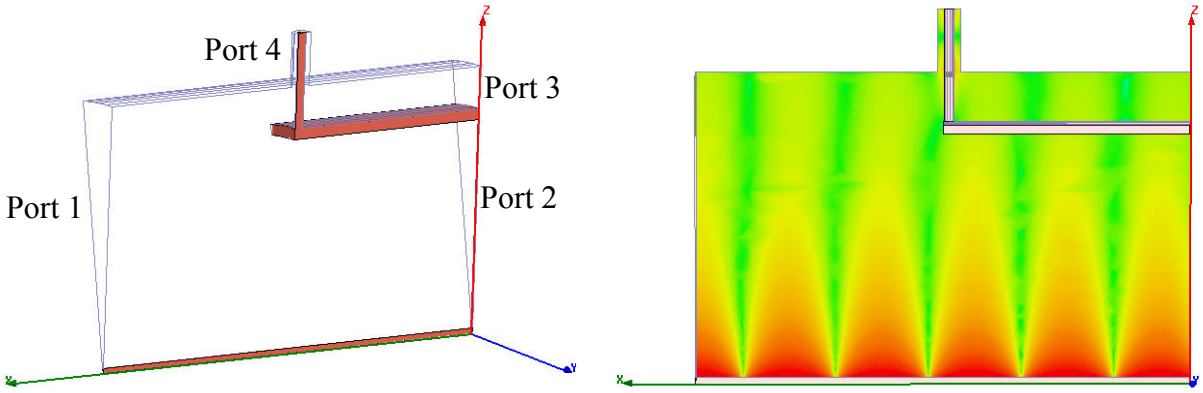

Fig. 11: Left: HFSS simulation of coaxial structure with 16 feedthroughs. A sector of 1/32 of the full structure was meshed. Right: Electric field at 20 GHz, logarithmic color scaling.

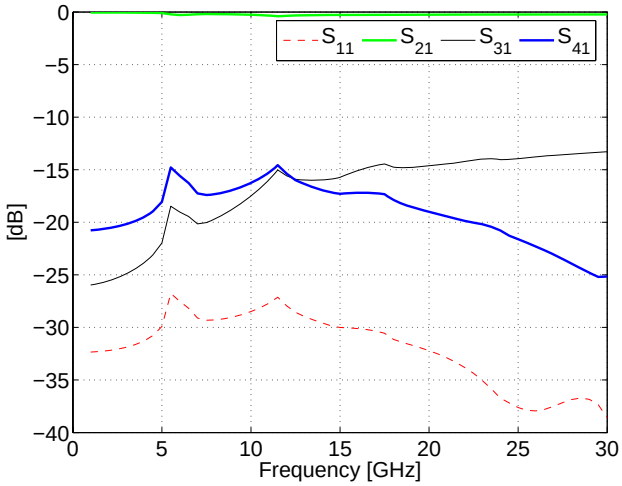

Fig. 12: S parameters of the coaxial section with 16 feedthroughs given in Fig. 11. S_{41} is combined signal coupled to the feedthroughs (thick blue trace).

Full structure

A realistic design combining the tapering, feedthrough and coaxial section was evaluated in HFSS (Fig. 13). The properties of the full structure are a combination of the tapering and feedthrough together. No significant new features were found. This means that the component-wise analysis is justified. Since the tapering introduces only resonances and a minor ripple, the full structure S_{41} is dominated by the feedthroughs. Again resonances appear at the cutoff of rotationally symmetric TM modes. Overall S_{41} is reasonably flat up to 20 GHz, where it starts to decrease due to the first azimuthal resonance that should appear at about 33 GHz, as found by scaling from Fig. 10.

Finally, Fig. 14 shows HFSS simulation results comparing the pick-up response of the full WCM structure for different taperings. Up to 10 GHz all curves are close together, indicating that the tapering does not have a big effect at low frequencies. At higher frequencies a much flatter response is obtained for sufficiently long taperings. The overall properties are very similar to the design without feedthroughs in Fig. 7.

For the structure with the 2 mm wide gap, it can be tried to find the high frequency cut-off using the quasi-static approach. The line impedance of the coaxial section is about 14 Ω, in parallel with 16 50 Ω lines this yields $R = 2.6\ \Omega$. Assuming a 2 mm wide ring-shaped capacitor with

2 mm plate distance, $C = 1.1$ pF. Equation 2 would then yield a cut-off frequency of 55 GHz. However, in this frequency range the quasi-static approach is not valid any more, as can be clearly seen from the simulation data.

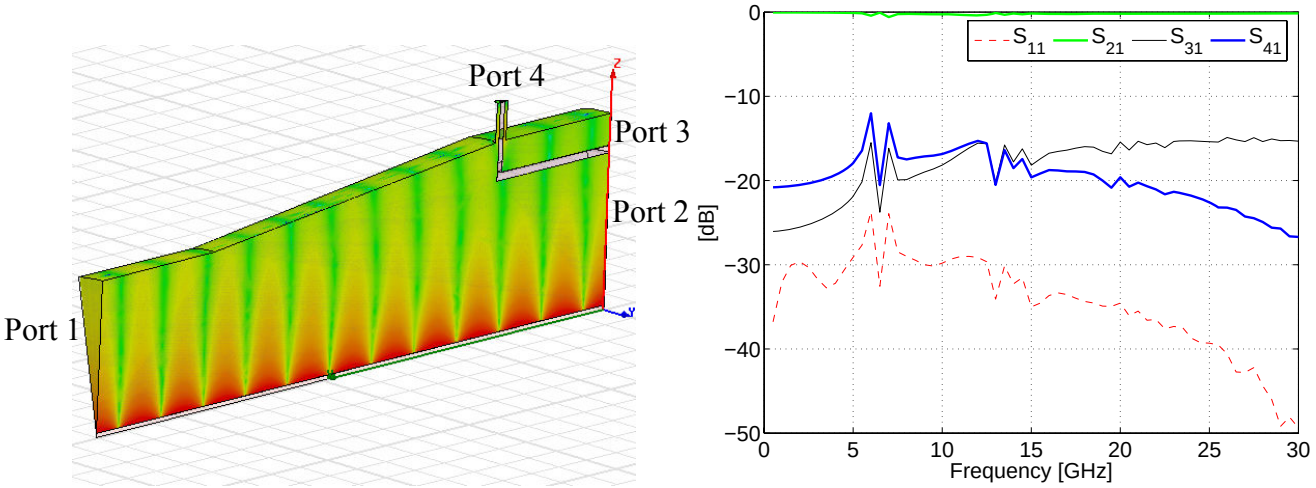

Fig. 13: Simulation of a combination of taper, feedthrough and coaxial section. Left: Electric field at 20 GHz. Right: S parameters of the structure.

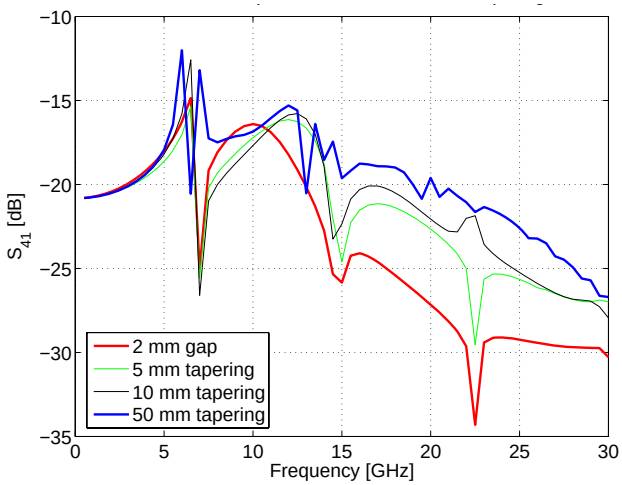

Fig. 14: HFSS Simulation results for the summed pick-up signal S_{41} for different taperings. The full WCM was modelled, including the tapering, (ideal) feedthroughs and the coaxial section as shown in Fig. 13. Up to about 10 GHz the curves do not differ much, which confirms that the quasi-static approximation is valid up to about this frequency. Above, the response deteriorates for designs with short taperings or a 2 mm gap.

4 Discussion

In this note the crucial RF properties of a wide band WCM were investigated. A number of points were not addressed and are left for further study [8].

- Ferrites and RF absorbers. In many designs in the literature ferrites are used to lower the WCM low-frequency cut-off *and* to absorb high frequency components. However, in addition to ferrites, dedicated RF absorbers could be used to improve the performance at very high frequencies [5]. In practise the RF absorbers can be installed in the coaxial section right after the feedthroughs. When the high frequency components are sufficiently damped, discontinuities can be introduced in the coaxial line without affecting much the high frequency properties. Ferrites to get the desired low frequency response can be

housed in a bigger cross-section coaxial line or a dielectric window can be installed before the ferrite. This could ease vacuum problems related to the outgassing of the ferrites

- Time domain response. Phase distortion in the WCM frequency response may lead to a distortion in the time domain response. Even though the phase looks close to linear in the HFSS frequency domain simulations, time domain codes with direct beam excitation such as GdfidL should be used as a cross-check.
- Wake fields. If there are significant discontinuities in the beam pipe close to the WCM, wake fields above beam pipe cut-off may reach the monitor. The WCM will detect these signal components, which may result in a significant increase in noise level. Microwave absorbing material upstream and downstream of the detector can be used to dampen such wake field signals [5].
- Damping of internal resonances. In particular at the cut-off of the TM_{01} mode at around 5.5 GHz the proposed design shows an enhanced response. Absorbing material inside the WCM structure might help to flatten these resonance peaks.
- Matching of feedthrough section. The response of the feedthrough section as shown in Fig. 11 and Fig. 12 can probably be improved by local matching of the feedthroughs. Modifications could look like the design used for low-reflection transitions between rectangular waveguides with TE_{10} modes and coaxial lines as described e.g. in [9]. Changing the longitudinal position of the feedthrough inner conductors or having them sit on dents protruding parallel to the beam pipe axis might also help.
- Offset beam. For beams offset from the center of the structure other modes than the rotationally symmetric TM_{0n} will be excited. Additional resonances leading to more ripple in the WCM response can be expected.
- Near field effects. The properties of the WCM may be improved by optimizing not only its components but the entire structure, including real feedthroughs.
- Aperture. Most of the problems related to resonances of waveguide mode cut-offs are mitigated by decreasing the radius of the coaxial structure. This way the resonances can be pushed to higher frequencies and eventually out of the band of interest. The same is the case for the azimuthal resonances, which allows to decrease the number of feedthroughs. However, decreasing the machine aperture may not be a viable option. In addition to that the mechanical implementation would get more tricky when the WCM is downscaled.

5 Conclusion

In this note an improved structure for a wall current monitor is presented. Due to the replacement of the longitudinal gap in existing designs by a coaxial structure the gap capacity is eliminated and the proposed design should have very high bandwidth. A flat frequency response up to at least 30 GHz was found in numerical simulations. However, when the tapering and feedthroughs are added, resonances appear that make the response more rugged, but its broad-band character remains.

Acknowledgements

I would like to thank Fritz Caspers, Lars Soby and Ivan Podadera and for numerous inspiring discussions and Elena Shaposhnikova and Trevor Linnecar for support.

References

1. Boussard, D; *Schottky noise and beam transfer function diagnostics*, CERN Accelerator School 1993 - p. 749-782, Geneva, 1993
2. Schulte, E; *Beam Position Monitors (Pick-Ups) and Q Measurement*, in: *Beam Instrumentation*, CERN-PE-ED-001-92, Geneva, 1992
3. Durand, J, Tardy T, Wurgel M; *A 10 GHz Wall Current Monitor*, CERN PS/LP Note 95-09, Geneva, 1995
4. Odier, P; *A New Wide Band Wall Current Monitor*, CERN-AB-2003-063-BDI, Geneva, 2003
5. Moore, C D; *Single Bunch Intensity Monitoring System Using an Improved Wall Current Monitor*, in: 13th IEEE Particle Accelerator Conference, USA, 1989
6. Vos, L, Very Wide Band Pick-ups, DIPAC'95, Lübeck-Travemünde, Germany, 1995
7. Durand, J, Tardy, T, Trabe, R; *A miniature ultrahigh vacuum feedthrough usable from DC to 20 GHz*, PS/LP note 96-09, Geneva, 1996
8. Podadera, I et al., *Status of the design of a wideband beam current monitor for EUROTEV*, to be published as EUROTeV-Report, 2006
9. Meinke, H, Gundlach, F W, *Taschenbuch der Hochfrequenztechnik*, Dritte Auflage, Springer, Berlin, 1968